

Article

# Particles in the Eluate from Double Filtration Plasmapheresis—A Case Study Using Field Emission Scanning Electron Microscopy/Energy-Dispersive X-ray Spectroscopy (FE-SEM/EDX)

Felix Scholkmann <sup>1,2,\*</sup>  and Antonietta M. Gatti <sup>3</sup>

<sup>1</sup> Biomedical Optics Research Laboratory, Department of Neonatology, University Hospital Zurich, University of Zurich, 8091 Zurich, Switzerland

<sup>2</sup> Scholkmann Data Analysis Services, Scientific Consulting and Physical Engineering, 8057 Zurich, Switzerland

<sup>3</sup> New Nanodiagnostics, San Vito, 41057 Modena, Italy

\* Correspondence: felix.scholkmann@usz.ch

**Abstract:** Unwanted substances can be effectively removed from the blood using double-filtration plasmapheresis (DFPP). In our case study, we used field emission scanning electron microscopy/energy-dispersive X-ray analysis (FE-SEM-EDX) to examine if the eluate obtained by a specific type of DFPP (INUSpheres with a TKM58 filter) contains nano- and microparticles and what chemical composition these particles have. We identified micro- and nanoparticles of various sizes and chemical composition, including microparticles high in the concentration of calcium, iron, silicon, aluminium and titanium. Furthermore, thread-like objects were identified. We discuss the possible origin of the particles and objects, their pathophysiological relevance and the potential of FE-SEM-EDX analysis of the eluate in terms of diagnostics and therapy for environmental medicine applications on patients.

**Keywords:** double-filtration plasmapheresis; INUSpheres; scanning electron microscopy/energy-dispersive X-ray analysis; FE-SEM-EDX; microparticles



**Citation:** Scholkmann, F.; Gatti, A.M. Particles in the Eluate from Double Filtration Plasmapheresis—A Case Study Using Field Emission Scanning Electron Microscopy/Energy-Dispersive X-ray Spectroscopy (FE-SEM/EDX). *Compounds* **2022**, *2*, 367–377. <https://doi.org/10.3390/compounds2040030>

Academic Editor: Jorge Pereira

Received: 8 September 2022

Accepted: 29 November 2022

Published: 1 December 2022

**Publisher's Note:** MDPI stays neutral with regard to jurisdictional claims in published maps and institutional affiliations.



**Copyright:** © 2022 by the authors. Licensee MDPI, Basel, Switzerland. This article is an open access article distributed under the terms and conditions of the Creative Commons Attribution (CC BY) license (<https://creativecommons.org/licenses/by/4.0/>).

## 1. Introduction

Double-filtration plasmapheresis (DFPP) enables removal of molecules/compounds/particles in blood plasma having sizes between the pore size of the first (plasma separator) and second filter membrane (plasma fractionator) [1]. The technique can remove pathophysiological relevant molecules (e.g., circulating immune complexes, circulating autoantigens, autoantibodies, damaged proteins) and toxic substances (e.g., environmental toxins) from the blood of a subject. DFPP has been successfully used therapeutically for the treatment of many diseases as a blood cleaning procedure [2], including rheumatoid arthritis [3–5], Guillain-Barré syndrome [6–10], multiple sclerosis [6,11–13], myasthenia gravis [6,14–19] and neuropathies [20–22]. A few years ago, a new type of DFPP (termed “INUSpheres”) was developed in Germany and its effectiveness was proven for example in the case of treating borreliosis [23], Alzheimer’s disease [24], peripheral neuropathy [25] and chronic post-COVID-19 syndrome (“long-COVID”) [26]. The application of DFPP (INUSpheres with a specific filter, TKM58) has been shown to change the blood composition; a recent study for example documented a decrease in the concentration of albumin,  $\gamma$ -globulins, triglycerides, total cholesterol, HDL-cholesterol, LDL-cholesterol, lipoprotein(a), ferritin, fibrinogen, IgG, IgM, IgA, total protein, INR, quick, platelets and an increase in erythrocytes, haematocrit and leukocytes [27].

Recently, we showed with near-infrared spectroscopy and the aquaphotomics approach that the water physicochemical properties (i.e., an increase in small water clusters, free water molecules and a decrease in hydroxylated water as well as superoxide in hydration shells) in the tissue change after DFPP treatment (INUSpheres with TKM58) [28].

Characteristic changes in the physicochemical water property of the eluate were also observed. Furthermore, we could document the presence of several toxins in the eluate, including aflatoxin B1, chromium, lead, cadmium, arsenic, lindane, cobalt, polycyclic-aromatic-hydrocarbons, disulfoton and aluminium (listed in descending concentration).

Since environmental pollution and human exposure to nano- and microparticles is a growing problem globally [29,30] with increasing evidence of their toxicity to humans [30–36], we hypothesised that the eluate would also contain these particles. In order to verify this experimentally, we carried out corresponding analysis of the eluate of a DFPPF application in one subject as a case study. Such an analysis has not been performed yet.

## 2. Materials and Methods

The first eluate obtained by a total of two DFPP treatments performed was used for the current study. The time between the two treatments was one day. The eluate resulted, as in the case of our previous study [28], from a DFPP INUSpheres (with TKM58 filter) treatments performed on a 39-year-old man (first author, FS) at a private clinic in Switzerland in February 2022. No official ethical approval was necessary to conduct the measurements and report the results since it is a case report (Kantonale Ethikkommission, Kanton Zürich, Switzerland) and measurements were done on an eluate sample from the first author (FS). The DFPP application was performed as part of a routine medical treatment.

Samples of the eluate obtained by the first and second DFPP treatment were screened for toxins (IGL Labor GmbH, Wittbek, Germany). To this end, the eluates in the infusion bags were shaken so that there was a homogeneous distribution of the components and then a sample (10 mL) of it was taken and sent to the analytical laboratory.

The eluate obtained from the first DFPP was filled in a 10 mL Vacutainer™ serum tube (with a silica (Si) based clot activator and gel for serum separation) and transferred from the side of collection (Switzerland) to the side of analysis (Italy). For the FE-SEM/EDX analysis a multiple sampling method was used: 20 µL of the fluid were pipetted from the upper, middle and bottom part of the vial (to distinguish different particle masses and particle volumes) and the samples were transferred on Millipore filters (0.45 µm pore size) for the FE-SEM/EDX analysis. The Millipore filters with the fluid samples were then placed on a carbon disc and deposited on the sample aluminium stub of the microscope. The samples were inserted in clean boxes and placed inside a thermostate at 30 °C for 30 min and afterwards analyzed with a FE-SEM (Quanta 650, Thermofisher, Waltham, MA, USA) equipped with an energy-dispersive X-ray (EDX) microprobe (Thermofischer, Waltham, MA, USA).

## 3. Results

As already reported in our previous publication [28], a variety of toxins were detected in the samples of the eluate of both DFPP treatments. Figure 1 shows the concentration of the metals detected with mass spectrometry. The concentrations were generally higher in the sample from the first DFPP compared to the second one. In the eluate sample of the first DFPP, aluminium (Al), arsenic (As), cadmium (Cd), chromium (Cr), cobalt (Co) and lead (Pb) were present in the concentration range from 400–600 nmol/L, and beryllium (Be), mercury (Hg), titanium (Ti) and zirconium (Zr) in the range from 0–400 nmol/L.

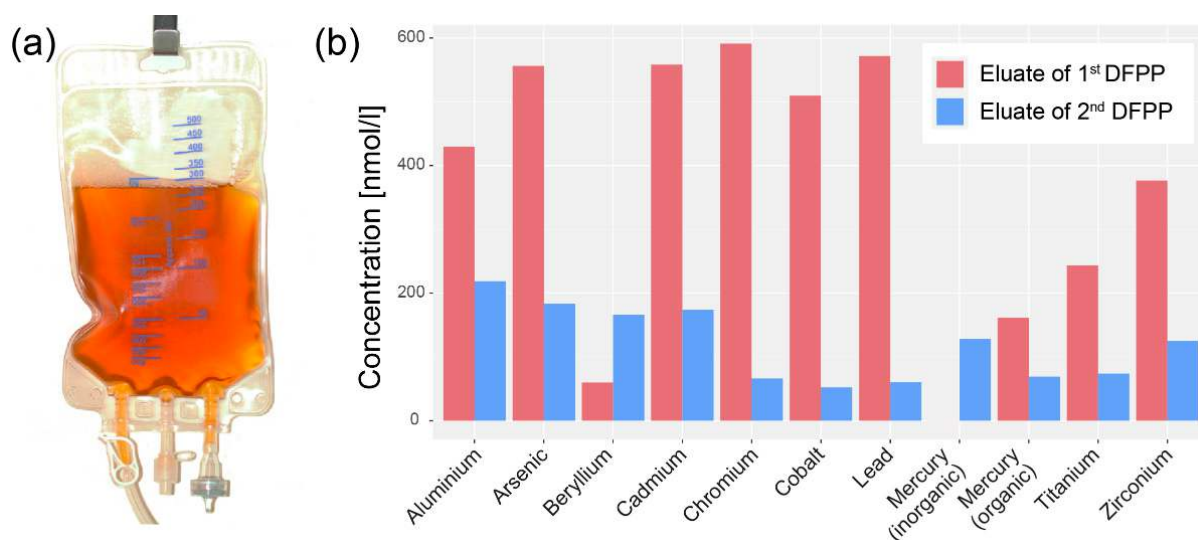


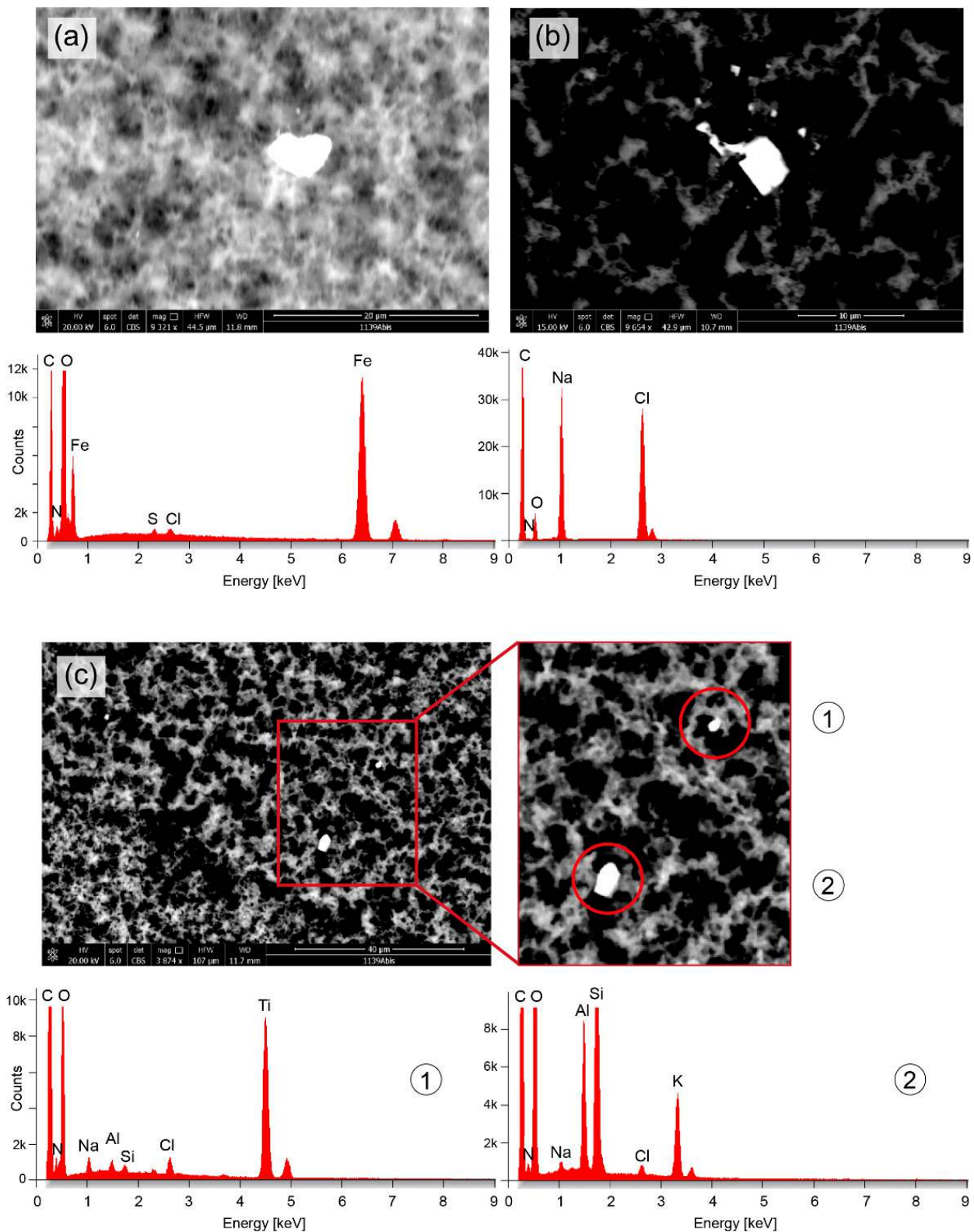
**Figure 1.** (a) Bag with eluate extracted during the first DFPP treatment. The colour of the eluate (yellowish-brown) illustrates the high concentration of filtered. (b) Concentration of metals detected in the two eluate samples (eluate from the first and second DFPP treatment; time between the two DFPP treatments: 1 day).

The FE-SEM/EDX analysis showed the presence of particulate matter with different chemical compositions from all three sampled regions of the eluate. The eluate sample from the bottom of the vial contained a large amount of aggregates in addition to the Si-based clot activator microparticles from the Vacutainer™ serum tube (characteristic and well-detectable ring-shaped cylinders with a diameter of about 10  $\mu\text{m}$ ). Most particles were found from the eluate sample of the upper part of the vial. Figures 2–4 show examples of the particles and objects found.

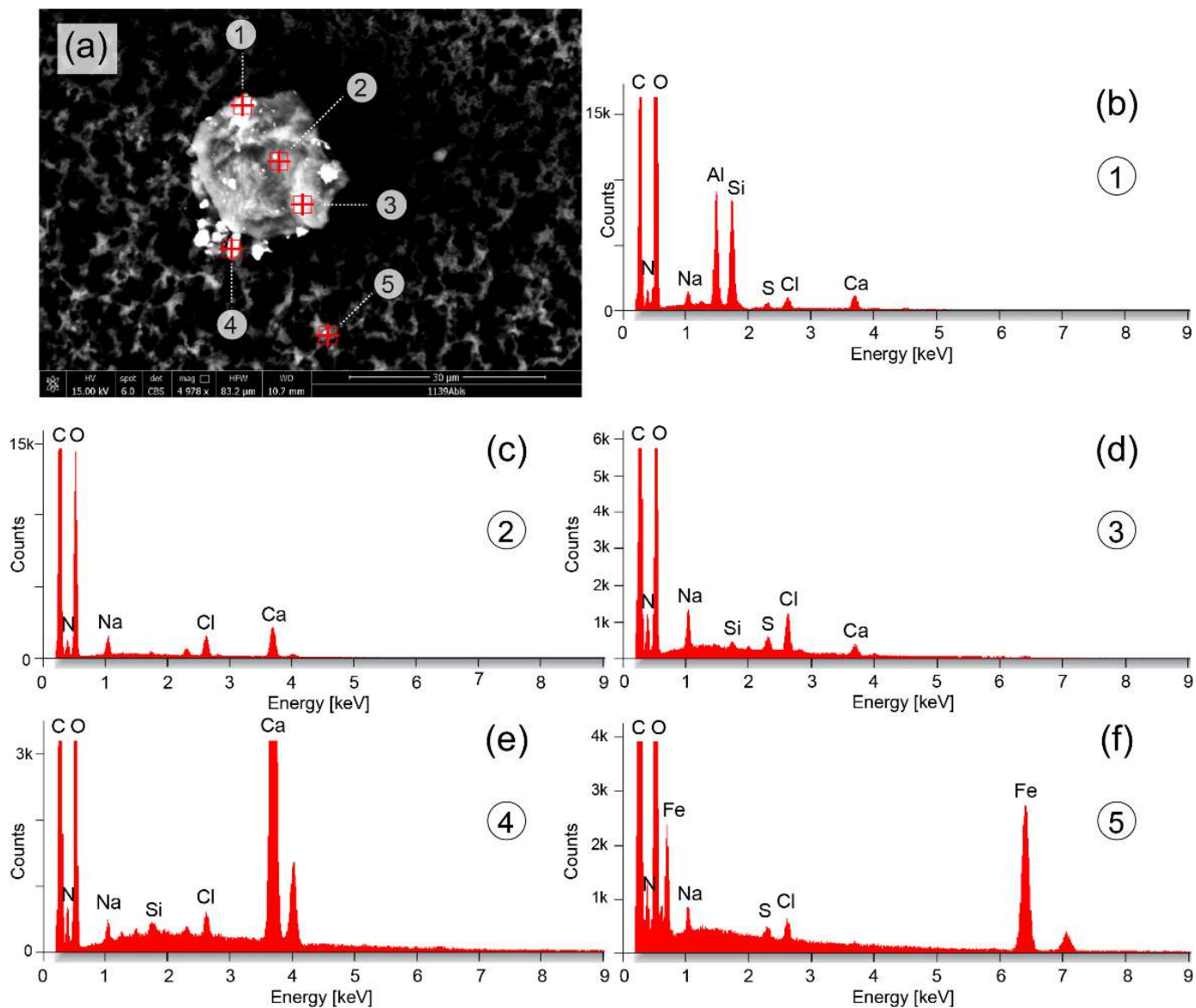
Figure 2 depicts the SEM images and EDX analysis results for four particles with sizes (diameter) of about 5  $\mu\text{m}$  (Figure 2a), 4  $\mu\text{m}$  (Figure 2b), 3  $\mu\text{m}$  and 1  $\mu\text{m}$  (Figure 3c). The particle shown in Figure 2a consist mainly of iron (Fe), the particle in Figure 2b of sodium (Na) and chloride (Cl), and the particles in Figure 2c of titanium (Ti) (particle #1) and a mixture of Si, Al and potassium (K) (particle #2).

Figure 3 shows a particle with a size of about 22  $\mu\text{m}$  with the presence of Na, Cl, Ca, Si and sulfur (S). Attached to the larger particle or nearby were smaller particles with sizes in the range of a few  $\mu\text{m}$  or nm. These particles comprise mainly Al and Si (Figure 3b), Ca (Figure 3e) or Fe (Figure 3f).

In Figure 4, elongated objects are depicted. The objects shown in Figure 4a,d,e were obtained from an eluate sample from the top part of the vial, those shown in Figure 4f,g from the middle part. The object in Figure 4a has a length of about 280  $\mu\text{m}$  and a diameter of about 9  $\mu\text{m}$ ; a smaller elongated object above the right end of the larger object has a length of about 50  $\mu\text{m}$ . Both objects consist mainly of Al, Na, Cl and S (Figure 4b,c). The object in Figure 4d was found to be thread-like, partially coiled, having a length of about 925  $\mu\text{m}$  and a diameter of about 7  $\mu\text{m}$ . Figure 4e shows an elongated and misshapen object (length: about 140  $\mu\text{m}$ , diameter: about 30  $\mu\text{m}$ ). On the surface of the objects shown in Figure 4d,e, nanoparticles (diameter: 0.5–150  $\mu\text{m}$ ) are visible. Figure 4f depicts another elongated thread-like object with as length of about 850  $\mu\text{m}$  and a diameter of 10–22  $\mu\text{m}$ . A similar object is shown in Figure 4g with a length of about 350  $\mu\text{m}$  and with a band-like structure (thickness in  $y$ -direction: about 2  $\mu\text{m}$ , thickness in  $z$ -direction: about 10  $\mu\text{m}$ ).



**Figure 2.** Microparticles detected in the upper part of the vial with the eluate. (a) Particle with a size (diameter) of about 5 μm (transverse length: 3.7 μm, vertical length: 6.4 μm) and a chemical composition mainly of Fe. (b) Particle with a size of about 4 μm (transverse length: 3.5 μm, vertical length: 4.7 μm) and a chemical composition mainly of Na and Cl. (c) Two particles (3 μm and 1 μm) comprising mainly Ti (particle #1) and a mixture of Si, Al and K (particle #2).



**Figure 3.** Microparticles detected in the upper part of the vial with the eluate. (a) Particle with a size (diameter) of about 22 μm and a chemical composition mainly of Na, Cl, Ca, Si and S (b–d). Smaller microparticles are attached to the larger particle or lay nearby, having sizes of about 4.5 μm (particle #1), 3 μm (particle #4) and 1.5 μm (particle #5). The chemical composition consists mainly of Al and Si (particle #1) (a), Ca (particle #4) (e) and Fe (particle #5) (f).

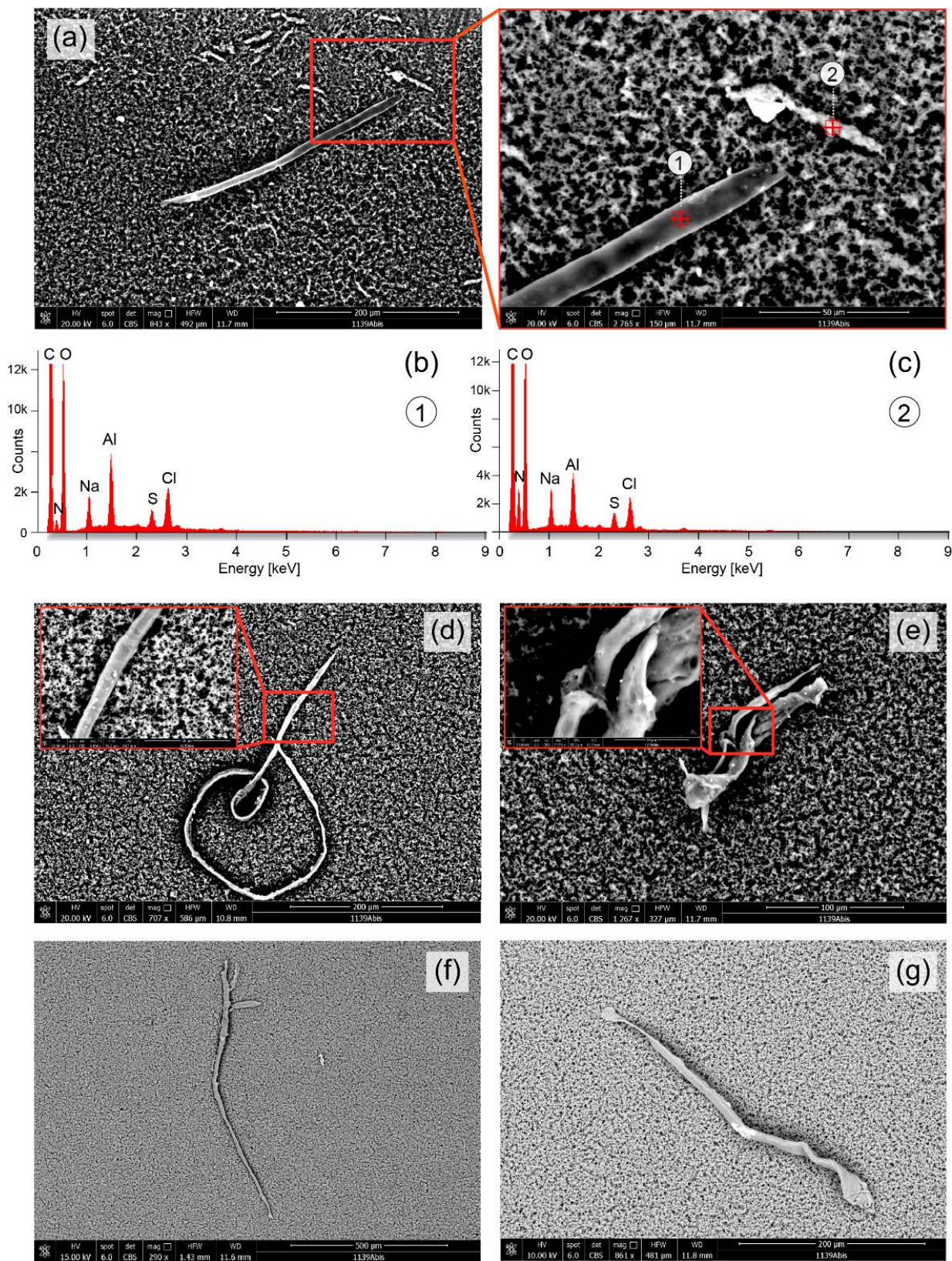


**Figure 4.** Elongated objects detected in the upper part (a,d,e) and middle part (f,g) of the vial with the eluate. (a) An object with a length of about 280  $\mu\text{m}$ , diameter of about 9  $\mu\text{m}$ , and a smaller particle nearby with a length of about 50  $\mu\text{m}$ . Both objects consisted mainly of Al, Na, Cl and S (b,c). (d) Further elongated objects detected with lengths of about 925  $\mu\text{m}$  (d), 140  $\mu\text{m}$  (e), 850  $\mu\text{m}$  (f) and 350  $\mu\text{m}$  (g). In the objects shown in (d,e), nanoparticles are visible on their surface.

#### 4. Discussion and Conclusions

In this study, we have shown that the eluate obtained by DFPP (INUSpheres with a TKM58 filter) contains organic and inorganic particulate matter. Particles and objects in the nano-to micrometre range were observed and characterized with the FE-SEM/EDX analysis.

The microparticles mainly consisting of Fe (Figures 2a and 3f) could be agglomerations of Fe from heme-containing biomolecules or free Fe due to hemolysis [33,34] or it can come from an environmental pollution (for example present in subway tunnels [37] or emitted by cars [38]).

The microparticle shown in Figure 2b consisting of mainly of Na and Cl is most probably a sodium chloride (NaCl) crystal due to the crystallization of Na and Cl present in the blood plasma (reference ranges: Na = 136–145 mmol/L, Cl = 98–106 mmol/L [35]).

The microparticle mainly composed of calcium (Ca) (Figure 3e) could be an agglomeration of Ca present in the plasma (normal concentration: 2.5 nmol/L [39]) which about half of it is bound to plasma proteins, e.g., albumin. Calcium carbonate ( $\text{CaCO}_3$ ) is also a food additive (E 170) (also in form of nanoparticles) [40] and in cosmetics [41], and calcium phosphate ( $\text{Ca}_3(\text{PO}_4)_2$ ) nanoparticles are widely used for introduction of DNA into eukaryotic cells (transfection) [42].

The big one from the two microparticles depicted in Figure 2c is a metal microparticle of Ti. It can be a Ti microparticle or a titanium dioxide ( $\text{TiO}_2$ ) microparticle.  $\text{TiO}_2$  microparticles are increasingly used in sunscreen [43]; however, their size is generally in the nm-range [44] and therefore smaller than the particle detected.  $\text{TiO}_2$  particles are also used as food additive (E171) [45], for example in seafood [46] or as a coating of chewing gums [47].  $\text{TiO}_2$  particles are also used as a non-stick coating in frying pans [48]. The size of  $\text{TiO}_2$  particles as food additive is also generally in the nm-range [49]. The source of the Ti or  $\text{TiO}_2$  particle found in the eluate is therefore not immediately clear as its size is in the  $\mu\text{m}$  range and not in the nm range as most of the industrially produced and used particles.

The microparticles containing Al and Si (Figures 2c and 3a [particle #1]) could be aluminium silicate (i.e.,  $x\text{Al}_2\text{O}_3 \cdot y\text{SiO}_2 \cdot z\text{H}_2\text{O}$ ) particles which are also used as a food additive (E559) [50]. Alternatively, they could have been formed in vivo or ex vivo (in the eluate between the end of the DFPP treatment and the analysis of it) through the synthesis of Si and Al available from other sources. Aluminium silicate is also part of the normal urban street dust [51]. Humans are increasingly exposed to Al [52,53] with food [54] and vaccines [55] as main sources. Further Al containing particles are the objects in Figure 4a. Both contain primarily Al, but no Si. The needle-like object (with a length of about 280  $\mu\text{m}$ ) is either primarily made of Al or contains an Al coating. Its origin is unknown since no description of a technical application of these kind of objects nor an environmental exposure source could be found in the literature. The same applies to the shorter Al-containing elongated shaped object in Figure 4a.

Concerning the thread-like objects in Figure 4, their source is not obvious. Preparation of the eluate samples were conducted under a laminar flow cabinet to avoid contamination with particles and filaments in the air and a specific protocol was used to perform the FE-SEM/EDX analysis in order to avoid any contamination of the sample and instrument. The thread-like object in Figure 4d, however, has a similar morphology and size as a thread-like parasitic nematode (roundworm) of the superfamily *Filarioridea* [56,57]. Different *Filarioridea* nematodes exist and can infect humans, including *Wuchereria bancrofti*, *Brugia malayi*, *Brugia timori*, *Onchocerca volvulus*, *Loa loa*, *Mansonella ozzardi*, *Mansonella perstans*, *Mansonella streptocerca* and *Brugia pahangi* [58]. Interestingly, the subject that underwent the DFPP treatment has been treated against chronic infections (*Borrelia afzelii*, *Borrelia burgdorferi* (CH), *Borrelia burgdorferi* (USA), *Borrelia garinii*, *Chlamydia pneumoniae*, *Babesia divergens*, *Bartonella henselae*, *Rickettsia Helvetica*, *Rickettsia conorii* and *Rickettsia helvetica*) months before. While the spirochetes *Borrelia* are larger than the thread-like object of Figure 4d, it could be a *Filarioridea* parasitic nematode indicating that the subject had also this kind of infection. It has been shown that ticks can be also infected with these filarial

nematodes [59,60]. There also the possibility that Figure 4f,g represent carbonious synthetic entities since the EDX spectrum is the same.

The amount of particles and objects detected in the eluate samples were less than expected based on the mass spectrometry results (Figure 1b) which indicated a large abundance of metals. This discrepancy might be explained by assuming that most of the metal in the eluate is present in nanoparticles and atoms/ions that were below the resolution of the FE-SEM used. It could be also that the bottom of the vial contained more of the metals than the middle or top part. However, due to the large presence of other inorganic and organic material as well as the Si coagulation agent particles at the bottom fraction, a dedicated analysis for nanoparticles could not be performed from this fraction. In future investigations of eluates, we plan to analyze also the bottom part in more detail by removing the organic biomolecules (by an enzymatic reaction) before FE-SEM/EDX analysis. In addition, transporting of the eluate without the Si-based clothing agent will be performed.

A clear limitation of our study is that our analysis is based on the eluate of one single person. Generalizations of our results are therefore only possible to a limited extent. The measurement of more eluate samples from different subjects was not aim of the present study since we wanted to test our FE-SEM/EDX approach first on samples from one subject (the first author) before conducting a study on a larger sample of subjects and eluates. This approach also had to be chosen due to the available financial budget, which for this pilot study only allowed the analysis that was carried out here. Our case study should (i) serve to document the feasibility to use the FE-SEM/EDX analysis approach to investigate the eluate obtained by DFPP, and (ii) stimulate further research on this topic. It should be investigated whether a FE-SEM/EDX analysis provides additional medically relevant information when a DFPP is performed. For example, specific detoxification protocols and medical treatments could be tailored to the amount and chemical composition of nano- and microparticles present in the eluate of a patient. The pollution of nano- and microparticles is an emerging health concern [32,61] and novel ways of quantifying the individual exposure as well as methods to remove these particles from the body are of imminent interest for preventing and treating human diseases. DFPP, possibly in combination with the application of chelating agents, might be a powerful way to remove these nano- and microparticles from the body. The analysis of the eluate with FE-SEM/EDX seems be a useful approach to proof this possibility.

In summary, our analysis of the eluate obtained from a DFPP application revealed particles and objects in the nm and  $\mu\text{m}$  range of different shape and chemical composition. Our study is the first to date to investigate the composition of an eluate obtained by DFPP with FE-SEM/EDX.

**Author Contributions:** Conceptualization, F.S. and A.M.G.; methodology, A.M.G. and F.S.; formal analysis, A.M.G. and F.S.; writing—original draft preparation, F.S.; writing—review and editing, A.M.G. and F.S.; visualization, F.S. All authors have read and agreed to the published version of the manuscript.

**Funding:** The FE-SEM/EDX analysis was financed by Karin Voit-Bak (INUS Medical Center AG, Germany). The two DFPP treatments were paid privately by the first author (F.S.).

**Institutional Review Board Statement:** Ethical review and approval were waived for this study since it is a case report and measurements were conducted with a sample provided by the first author (FS). The DFPP treatment was performed as part of a routine medical treatment.

**Informed Consent Statement:** Not applicable.

**Data Availability Statement:** The data will be made available by the corresponding author, upon reasonable request.

**Acknowledgments:** We thank Rachel Scholkmann for English proofreading.

**Conflicts of Interest:** The authors declare no conflict of interest.

## References

1. Agishi, T.; Kaneko, I.; Hasuo, Y.; Hayasaka, Y.; Sanaka, T.; Ota, K.; Amemiya, H.; Sugino, N.; Abe, M.; Ono, T.; et al. Double Filtration Plasmapheresis. *ASAIO J.* **1980**, *26*, 406–411. [[CrossRef](#)]
2. Hirano, R.; Namazuda, K.; Hirata, N. Double filtration plasmapheresis: Review of current clinical applications. *Ther. Apher. Dial.* **2020**, *25*, 145–151. [[CrossRef](#)] [[PubMed](#)]
3. Yu, X.; Ma, J.; Tian, J.; Jiang, S.; Xu, P.; Han, H.; Wang, L. A Controlled Study of Double Filtration Plasmapheresis in the Treatment of Active Rheumatoid Arthritis. *JCR J. Clin. Rheumatol.* **2007**, *13*, 193–198. [[CrossRef](#)] [[PubMed](#)]
4. Matsuda, Y.; Tsuda, H.; Takasaki, Y.; Hashimoto, H. Double Filtration Plasmapheresis for the Treatment of a Rheumatoid Arthritis Patient with Extremely High Level of C-reactive Protein. *Ther. Apher. Dial.* **2004**, *8*, 404–408. [[CrossRef](#)] [[PubMed](#)]
5. Liu, J.-D.; Zhang, C.; Li, W.-S.; Lun, L.-D. Double Filtration Plasmapheresis for the Treatment of Rheumatoid Arthritis: A Study of 21 Cases. *Artif. Organs* **2008**, *21*, 96–98. [[CrossRef](#)] [[PubMed](#)]
6. Ito, Y.; Odaka, M.; Tabata, Y.; Soeda, K.; Hayashi, H.; Kobayashi, S.; Sato, T.; Yamane, S.; Isono, K. Clinical Experience of Double Filtration Plasmapheresis for Drug Refractory Neurological Diseases. *Biomater. Artif. Cells Immobil. Biotechnol.* **2009**, *19*, 27–35. [[CrossRef](#)]
7. Lyu, R.-K.; Chen, W.-H.; Hsieh, S.-T. Plasma Exchange Versus Double Filtration Plasmapheresis in the Treatment of Guillain-Barre Syndrome. *Ther. Apher. Dial.* **2002**, *6*, 163–166. [[CrossRef](#)]
8. Lin, J.-H.; Tu, K.-H.; Chang, C.-H.; Chen, Y.-C.; Tian, Y.-C.; Yu, C.-C.; Hung, C.-C.; Fang, J.-T.; Yang, C.-W.; Chang, M.-Y. Prognostic factors and complication rates for double-filtration plasmapheresis in patients with Guillain-Barré syndrome. *Transfus. Apher. Sci.* **2015**, *52*, 78–83. [[CrossRef](#)]
9. Cheng, B.-C.; Chang, W.-N.; Chen, J.-B.; Chee, E.C.-Y.; Huang, C.-R.; Lu, C.-H.; Chang, C.-J.; Hung, P.-L.; Chuang, Y.-C.; Lee, C.-T.; et al. Long-term prognosis for Guillain-Barré syndrome: Evaluation of prognostic factors and clinical experience of automated double filtration plasmapheresis. *J. Clin. Apher.* **2003**, *18*, 175–180. [[CrossRef](#)]
10. Chen, W.-H.; Yeh, J.-H.; Chiu, H.-C. Experience of double filtration plasmapheresis in the treatment of Guillain-Barre syndrome. *J. Clin. Apher.* **1999**, *14*, 126–129. [[CrossRef](#)]
11. Ramunni, A.; De Robertis, F.; Brescia, P.; Saliani, M.T.; Amoroso, M.; Prontera, M.; Dimonte, E.; Trojano, M.; Coratelli, P. A Case Report of Double Filtration Plasmapheresis in an Acute Episode of Multiple Sclerosis. *Ther. Apher. Dial.* **2008**, *12*, 250–254. [[CrossRef](#)]
12. De Masi, R.; Orlando, S.; Accoto, S. Double Filtration Plasmapheresis Treatment of Refractory Multiple Sclerosis Relapsed on Fingolimod: A Case Report. *Appl. Sci.* **2020**, *10*, 7404. [[CrossRef](#)]
13. Matsuo, H. Plasmapheresis in acute phase of multiple sclerosis and neuromyelitis optica. *Nihon Rinsho. Jpn. J. Clin. Med.* **2014**, *72*, 1999–2002.
14. Yeh, J.-H.; Chiu, H.-C. Comparison between double-filtration plasmapheresis and immunoadsorption plasmapheresis in the treatment of patients with myasthenia gravis. *J. Neurol.* **2000**, *247*, 510–513. [[CrossRef](#)] [[PubMed](#)]
15. Bennani, H.N.; Lagrange, E.; Noble, J.; Malvezzi, P.; Motte, L.; Chevallier, E.; Rostaing, L.; Jouve, T. Treatment of refractory myasthenia gravis by double-filtration plasmapheresis and rituximab: A case series of nine patients and literature review. *J. Clin. Apher.* **2020**, *36*, 348–363. [[CrossRef](#)]
16. Liu, J.-F.; Wang, W.-X.; Xue, J.; Zhao, C.-B.; You, H.-Z.; Lu, J.-H.; Gu, Y. Comparing the Autoantibody Levels and Clinical Efficacy of Double Filtration Plasmapheresis, Immunoadsorption, and Intravenous Immunoglobulin for the Treatment of Late-onset Myasthenia Gravis. *Ther. Apher. Dial.* **2010**, *14*, 153–160. [[CrossRef](#)]
17. Zhang, L.; Liu, J.; Wang, H.; Zhao, C.; Lu, J.; Xue, J.; Gu, Y.; Hao, C.; Lin, S.; Lv, C. Double filtration plasmapheresis benefits myasthenia gravis patients through an immunomodulatory action. *J. Clin. Neurosci.* **2014**, *21*, 1570–1574. [[CrossRef](#)]
18. Yeh, J.H.; Chiu, H.C. Double filtration plasmapheresis in myasthenia gravis-analysis of clinical efficacy and prognostic parameters. *Acta Neurol. Scand.* **2009**, *100*, 305–309. [[CrossRef](#)]
19. Yeh, J.H.; Chen, W.H.; Chiu, H.C. Double filtration plasmapheresis in the treatment of myasthenic crisis-analysis of prognostic factors and efficacy. *Acta Neurol. Scand.* **2001**, *104*, 78–82. [[CrossRef](#)]
20. Podestà, M.A.; Gennarini, A.; Portalupi, V.; Rota, S.; Alessio, M.G.; Remuzzi, G.; Ruggenti, P. Accelerating the Depletion of Circulating Anti-Phospholipase A<sub>2</sub> Receptor Antibodies in Patients with Severe Membranous Nephropathy: Preliminary Findings with Double Filtration Plasmapheresis and Ofatumumab. *Nephron* **2020**, *144*, 30–35. [[CrossRef](#)]
21. Chiu, H.-C.; Chen, W.-H.; Yeh, J.-H. Double Filtration Plasmapheresis in the Treatment of Inflammatory Polyneuropathy. *Ther. Apher.* **1997**, *1*, 183–186. [[CrossRef](#)] [[PubMed](#)]
22. Kumazawa, K.; Yuasa, N.; Mitsuma, T.; Nagamatsu, M.; Sobue, G. Double filtration plasmapheresis (DFPP) in chronic inflammatory demyelinating polyradiculoneuropathy (CIDP). *Rinsho Shinkeigaku = Clin. Neurol.* **1998**, *38*, 719–723.
23. Straube, R.; Voit-Bak, K.; Gor, A.; Steinmeier, T.; Chrousos, G.P.; Boehm, B.O.; Birkenfeld, A.L.; Barbir, M.; Balanzew, W.; Bornstein, S.R. Lipid Profiles in Lyme Borreliosis: A Potential Role for Apheresis? *Horm. Metab. Res.* **2019**, *51*, 326–329. [[CrossRef](#)] [[PubMed](#)]
24. Bornstein, S.R.; Voit-Bak, K.; Rosenthal, P.; Tselmin, S.; Julius, U.; Schatz, U.; Boehm, B.O.; Thuret, S.; Kempermann, G.; Reichmann, H.; et al. Extracorporeal apheresis therapy for Alzheimer disease—Targeting lipids, stress, and inflammation. *Mol. Psychiatry* **2019**, *25*, 275–282. [[CrossRef](#)]

25. Straube, R.; Müller, G.; Voit-Bak, K.; Tselmin, S.; Julius, U.; Schatz, U.; Rietzsch, H.; Reichmann, H.; Chrousos, G.P.; Schürmann, A.; et al. Metabolic and Non-Metabolic Peripheral Neuropathy: Is there a Place for Therapeutic Apheresis? *Horm. Metab. Res.* **2019**, *51*, 779–784. [[CrossRef](#)]
26. Bornstein, S.R.; Voit-Bak, K.; Donate, T.; Rodionov, R.N.; Gainetdinov, R.R.; Tselmin, S.; Kanczkowski, W.; Müller, G.M.; Achleitner, M.; Wang, J.; et al. Chronic post-COVID-19 syndrome and chronic fatigue syndrome: Is there a role for extracorporeal apheresis? *Mol. Psychiatry* **2021**, *27*, 34–37. [[CrossRef](#)]
27. Yin, X.; Takov, K.; Straube, R.; Voit-Bak, K.; Graessler, J.; Julius, U.; Tselmin, S.; Rodionov, R.; Barbir, M.; Walls, M.; et al. Precision Medicine Approach for Cardiometabolic Risk Factors in Therapeutic Apheresis. *Horm. Metab. Res. = Horm.-Und Stoffwechs. = Horm. Et Metab.* **2022**, *54*, 238–249. [[CrossRef](#)]
28. Scholkmann, F.; Tsenkova, R. Changes in Water Properties in Human Tissue after Double Filtration Plasmapheresis-A Case Study. *Molecules* **2022**, *27*, 3947. [[CrossRef](#)]
29. Dwivedi, A.D.; Dubey, S.P.; Sillanpää, M.; Kwon, Y.-N.; Lee, C.; Varma, R.S. Fate of engineered nanoparticles: Implications in the environment. *Coord. Chem. Rev.* **2015**, *287*, 64–78. [[CrossRef](#)]
30. Mitrano, D.M.; Wick, P.; Nowack, B. Placing nanoplastics in the context of global plastic pollution. *Nat. Nanotechnol.* **2021**, *16*, 491–500. [[CrossRef](#)]
31. Lungu, M.; Neculae, A.; Bunoiu, M.; Biris, C. Nanoparticles' Promises and Risks. In *Nanoparticles' Promises and Risks: Characterization, Manipulation, and Potential Hazards to Humanity and the Environment*; Springer: Berlin/Heidelberg, Germany, 2015. [[CrossRef](#)]
32. Gatti, A.M.; Montanari, S. *Nanopathology: The Nano-Bio-Interaction of Nanoparticles Inside the Human Body*; Springer: Cham, Switzerland, 2015; pp. 71–85. [[CrossRef](#)]
33. Vallelian, F.; Buehler, P.W.; Schaer, D.J. Hemolysis, free hemoglobin toxicity and scavenger protein therapeutics. *Blood* **2022**, *140*, 1837–1844. [[CrossRef](#)] [[PubMed](#)]
34. Schaer, D.J.; Buehler, P.W.; Alayash, A.I.; Belcher, J.D.; Vercellotti, G.M. Hemolysis and free hemoglobin revisited: Exploring hemoglobin and hemin scavengers as a novel class of therapeutic proteins. *Blood* **2013**, *121*, 1276–1284. [[CrossRef](#)] [[PubMed](#)]
35. MSD-Manual. Representative Laboratory Reference Values: Blood, Plasma, and Serum. Available online: <https://www.msmanuals.com/professional/multimedia/table/representative-laboratory-reference-values-blood-plasma-and-serum> (accessed on 8 September 2022).
36. Sonwani, S.; Madaan, S.; Arora, J.; Suryanarayan, S.; Rangra, D.; Mongia, N.; Vats, T.; Saxena, P. Inhalation Exposure to Atmospheric Nanoparticles and Its Associated Impacts on Human Health: A Review. *Front. Sustain. Cities* **2021**, *3*, 690444. [[CrossRef](#)]
37. Lee, Y.; Lee, Y.-C.; Kim, T.; Choi, J.; Park, D. Sources and Characteristics of Particulate Matter in Subway Tunnels in Seoul, Korea. *Int. J. Environ. Res. Public Health* **2018**, *15*, 2534. [[CrossRef](#)]
38. Golokhvast, K.S.; Chernyshev, V.V.; Chaika, V.V.; Ugay, S.M.; Zelinskaya, E.V.; Tsatsakis, A.M.; Karakitsios, S.P.; Sarigiannis, D.A. Size-segregated emissions and metal content of vehicle-emitted particles as a function of mileage: Implications to population exposure. *Environ. Res.* **2015**, *142*, 479–485. [[CrossRef](#)]
39. Lester, E.; Varghese, Z. Differences in the calcium concentration of serum and plasma initially and after storage. *Ann. Clin. Biochem.* **1977**, *14*, 39–44. [[CrossRef](#)]
40. Efsa Panel on Food Contact Materials; Enzymes and Processing Aids; Lambre, C.; Barat Baviera, J.M.; Bolognesi, C.; Chesson, A.; Cocconcelli, P.S.; Crebelli, R.; Gott, D.M.; Grob, K.; et al. Safety assessment of the substance nano precipitated calcium carbonate for use in plastic food contact materials. *EFSA J. Eur. Food Saf. Auth.* **2022**, *20*, e07135. [[CrossRef](#)]
41. Carella, F.; Degli Esposti, L.; Adamiano, A.; Iafisco, M. The Use of Calcium Phosphates in Cosmetics, State of the Art and Future Perspectives. *Materials* **2021**, *14*, 6398. [[CrossRef](#)]
42. Kwon, M.; Firestein, B.L. DNA transfection: Calcium phosphate method. *Methods Mol. Biol.* **2013**, *1018*, 107–110. [[CrossRef](#)]
43. Trivedi, M.; Murase, J. Titanium Dioxide in Sunscreen. In *Application of Titanium Dioxide*; Janus, M., Ed.; IntechOpen: London, UK, 2017. [[CrossRef](#)]
44. Lewicka, Z.A.; Benedetto, A.F.; Benoit, D.N.; Yu, W.W.; Fortner, J.D.; Colvin, V.L. The structure, composition, and dimensions of TiO<sub>2</sub> and ZnO nanomaterials in commercial sunscreens. *J. Nanopart. Res.* **2011**, *13*, 3607–3617. [[CrossRef](#)]
45. Ropers, M.-H.; Terrisse, H.; Mercier-Bonin, M.; Humbert, B. Titanium Dioxide as Food Additive. In *Application of Titanium Dioxide*; Janus, M., Ed.; IntechOpen: London, UK, 2017.
46. Yin, C.; Zhao, W.; Liu, R.; Liu, R.; Wang, Z.; Zhu, L.; Chen, W.; Liu, S. TiO<sub>2</sub> particles in seafood and surimi products: Attention should be paid to their exposure and uptake through foods. *Chemosphere* **2017**, *188*, 541–547. [[CrossRef](#)] [[PubMed](#)]
47. Dufefoi, W.; Terrisse, H.; Popa, A.F.; Gautron, E.; Humbert, B.; Ropers, M.-H. Evaluation of the content of TiO<sub>2</sub> nanoparticles in the coatings of chewing gums. *Food Addit. Contam. Part A* **2017**, *35*, 211–221. [[CrossRef](#)] [[PubMed](#)]
48. Golja, V.; Dražić, G.; Lorenzetti, M.; Vidmar, J.; Ščančar, J.; Zalaznik, M.; Kalin, M.; Novak, S. Characterisation of food contact non-stick coatings containing TiO<sub>2</sub> nanoparticles and study of their possible release into food. *Food Addit. Contam. Part A* **2017**, *34*, 421–433. [[CrossRef](#)] [[PubMed](#)]
49. Weir, A.; Westerhoff, P.; Fabricius, L.; Hristovski, K.; von Goetz, N. Titanium dioxide nanoparticles in food and personal care products. *Environ. Sci. Technol.* **2012**, *46*, 2242–2250. [[CrossRef](#)] [[PubMed](#)]

50. EFSA. *Dietary Exposure to Aluminium-Containing Food Additives*; European Food Safety Authority, EFSA Supporting Publications: Parma, Italy, 2013; Volume 10. [[CrossRef](#)]
51. El-Zahhar, A.A.; Idris, A.M.; Fawy, K.F.; Arshad, M. SEM, SEM-EDX,  $\mu$ -ATR-FTIR and XRD for urban street dust characterisation. *Int. J. Environ. Anal. Chem.* **2019**, *101*, 988–1006. [[CrossRef](#)]
52. Exley, C. Human exposure to aluminium. *Environ. Sci. Process. Impacts* **2013**, *15*, 1807–1816. [[CrossRef](#)]
53. Wong, W.W.; Chung, S.W.; Kwong, K.P.; Yin Ho, Y.; Xiao, Y. Dietary exposure to aluminium of the Hong Kong population. *Food Addit. Contam. Part A Chem. Anal. Control. Expo. Risk Assess.* **2010**, *27*, 457–463. [[CrossRef](#)]
54. Paz, S. Aluminium Exposure Through the Diet. *Food Sci. Nutr.* **2017**, *3*, 1–10. [[CrossRef](#)]
55. McFarland, G.; La Joie, E.; Thomas, P.; Lyons-Weiler, J. Acute exposure and chronic retention of aluminum in three vaccine schedules and effects of genetic and environmental variation. *J. Trace Elem. Med. Biol.* **2020**, *58*, 126444. [[CrossRef](#)]
56. Lu, I.M.; Kassis, T.; Rogers, A.M.; Schudel, A.; Weil, J.; Evans, C.C.; Moorhead, A.R.; Thomas, S.N.; Dixon, J.B. Optimization of culture and analysis methods for enhancing long-term *Brugia malayi* survival, molting and motility in vitro. *Parasitol. Open* **2018**, *4*, e3. [[CrossRef](#)]
57. Oliveira-Menezes, A.; Lins, R.; Noroes, J.; Dreyer, G.; Lanfredi, R.M. Comparative analysis of a chemotherapy effect on the cuticular surface of *Wuchereria bancrofti* adult worms in vivo. *Parasitol. Res.* **2007**, *101*, 1311–1317. [[CrossRef](#)] [[PubMed](#)]
58. Paily, K.P.; Hoti, S.L.; Das, P.K. A review of the complexity of biology of lymphatic filarial parasites. *J. Parasit. Dis. Off. Organ Indian Soc. Parasitol.* **2009**, *33*, 3–12. [[CrossRef](#)] [[PubMed](#)]
59. Namrata, P.; Miller, J.; Shilpa, M.; Reddy, P.; Bandoski, C.; Rossi, M.; Sapi, E. Filarial Nematode Infection in Ixodes scapularis Ticks Collected from Southern Connecticut. *Vet. Sci.* **2014**, *1*, 5–15. [[CrossRef](#)]
60. Henning, T.C.; Orr, J.M.; Smith, J.D.; Arias, J.R.; Rasgon, J.L.; Norris, D.E. Discovery of filarial nematode DNA in *Amblyomma americanum* in Northern Virginia. *Ticks Tick-Borne Dis.* **2016**, *7*, 315–318. [[CrossRef](#)] [[PubMed](#)]
61. Kreyling, W.G.; Semmler-Behnke, M.; Möller, W. Health implications of nanoparticles. *J. Nanopart. Res.* **2006**, *8*, 543–562. [[CrossRef](#)]